MASSIVELY PARALLEL ELECTRICAL CONDUCTIVITY IMAGING OF THE SUBSURFACE: APPLICATIONS TO HYDROCARBON EXPLORATION

Gregory A Newman and Michael Commer
Lawrence Berkeley National Laboratory, MS-90-1116 Berkeley Ca, 94720
ganewman@lbl.gov

ABSTRACT

Three-dimensional (3D) geophysical imaging is now receiving considerable attention for electrical conductivity mapping of potential offshore oil and gas reservoirs. The imaging technology employs controlled source electromagnetic (CSEM) and magnetotelluric (MT) fields and treats geological media exhibiting transverse anisotropy. Moreover when combined with established seismic methods, direct imaging of reservoir fluids is possible. Because of the size of the 3D conductivity imaging problem, strategies are required exploiting computational parallelism and optimal meshing. The algorithm thus developed has been shown to scale to tens of thousands of processors. In one imaging experiment, 32,768 tasks/processors on the IBM Watson Research Blue Gene/L supercomputer were successfully utilized. Over a 24 hour period we were able to image a large scale field data set that previously required over four months of processing time on distributed clusters based on Intel or AMD processors utilizing 1024 tasks on an InfiniBand fabric. Electrical conductivity imaging using massively parallel computational resources produces results that cannot be obtained otherwise and are consistent with timeframes required for practical exploration problems.

1. Introduction

Seismic imaging methods have a long and established history in hydrocarbon reservoir exploration. Yet the technology has encountered difficulty in discriminating different types of reservoir fluids, such as brines, oil, and gas. This limitation has led to the development of new geophysical technologies, specifically the use of low-frequency electromagnetic energy to complement seismic methods. In contrast to seismic data, electromagnetic measurements have shown to be highly sensitive to changes in fluid types and hence the location of hydrocarbons. Among such measurement techniques, the key emergent EM technology with respect to hydrocarbon exploration is controlled source electromagnetics (CSEM). CSEM utilizes low-frequency EM energy (less than 1 Hz) to map variations in the subsurface electrical conductivity, σ (in units of Siemens per meter, (S/m)) or its reciprocal ($1/\sigma$ in units of ohm-meters, (Ω.m)), called resistivity [1, 2, 3]. CSEM measurements are carried out using a deep-towed transmitter to excite low-frequency electromagnetic signals. The signals are measured on the sea floor by electric and magnetic field sensors/detectors with the largest transmitter-detector separations exceeding 15 km (Figure 1). The method can interrogate down to 4 km depth, below the seabed. Another relevant EM technology employs natural field emissions below 0.1 Hz that arise from the interaction of the solar wind with the Earth's magnetosphere. Previously considered a source of noise when measuring CSEM fields, magnetotelluric (MT) fields complement CSEM measurements. Though not sensitive to oil bearing formations, MT fields are sensitive to electrical resistivity variations on a gross scale and interrogate to greater depths than the CSEM method. A consensus is now emerging that MT data can significantly help in reducing uncertainty and ambiguity in interpreting CSEM data [4, 5].

Successfully extracting and processing the information from electromagnetic CSEM and MT data has proved up to now to be a formidable problem. The problem is especially significant in the search for hydrocarbon energy in highly complex *offshore* geological environments, where many of the world's oil and gas deposits remain to be found. Such offshore hydrocarbon exploration is an especially arduous task because reservoirs generally reside in highly complex geological environments, often beneath miles of ocean. Deep-water reservoirs are exceedingly difficult to successfully locate without recourse to imaging them and the background geology in three spatial dimensions (3D). To provide a maximally consistent electromagnetic data interpretation to geologists, such imaging requires large-scale modeling, spatially exhaustive survey coverage, and multi-component data volumes. Moreover it is now recognized that the

3D conductivity imaging of marine CSEM data is strongly influenced by electrical anisotropy of geological media [4, 7, 8]. Failure to treat such effects in the imaging processes can produce misleading results. To effectively deal with the problem it is necessary to incorporate anisotropy within the 3D imaging framework. Here we discuss one such approach that treats transverse anisotropy, which appears to be relevant for many exploration scenarios.

The 3D imaging problem, which in this paper is also referred to as the inversion problem, usually has large computational demands, due to the computationally expensive solution of the forward modeling problem of EM field simulation on a given 3D finite-difference (FD) grid. It is described by a sparse linear system of equations that is solved using iterative Krylov methods. Such methods readily parallelize and are straight forward to implement. However, large data volumes require many forward solutions in an iterative inversion scheme. Therefore, we have developed an imaging algorithm that utilizes two levels of parallelization, one applied to the modeling, or imaging, volume and the other applied to the data volume. The algorithm is designed for arbitrarily large datasets, allowing for an arbitrarily large number of parallel tasks, while the computationally idle message passing is minimized. We have further incorporated an optimal meshing scheme that allows us to separate the imaging or modeling mesh from the simulation mesh [9]. This provides for significant acceleration of the 3D EM field simulation, having a direct impact on the time to solution for the 3D imaging process. Much of the details of the 3D imaging approach adopted in this paper have been published elsewhere for the isotropic media [9, 10]. Extension to treat media exhibiting transverse anisotropy is straight forward [6].

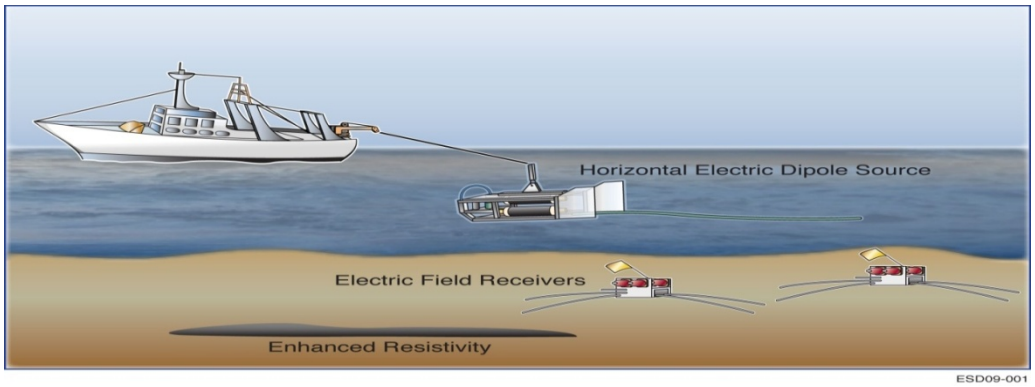

Figure 1. The CSEM technique senses regions of enhanced resistivity that can be associated with oil or gas deposits. This technique interrogates down to reservoir depths (as deep as 4 km beneath the ocean floor with the current technology). Sea bottom receivers are also used to collect natural field (MT) data.

2. Minimization Procedure

We seek to minimize the error functional

$$\phi = \tfrac{1}{2}\{\mathbf{D}_{CSEM}(\mathbf{d}^{p} - \mathbf{d}^{obs})^{T^*}\{\mathbf{D}_{CSEM}(\mathbf{d}^{p} - \mathbf{d}^{obs})\}(\alpha) + \tfrac{1}{2}\{\mathbf{D}_{MT}(\mathbf{Z}^{p} - \mathbf{Z}^{obs})^{T^*}\{\mathbf{D}_{MT}(\mathbf{Z}^{p} - \mathbf{Z}^{obs})\}(\beta) + \tfrac{1}{2}\lambda_h\{\mathbf{W}\mathbf{m}_h\}^{T}\{\mathbf{W}\mathbf{m}_h\} + \tfrac{1}{2}\lambda_v\{\mathbf{W}\mathbf{m}_v\}^{T}\{\mathbf{W}\mathbf{m}_v \quad (1)$$

$\mathbf{T}^*$ denotes the transpose-conjugation operator and $\mathbf{d}^{obs}$ and $\mathbf{d}^{p}$ the observed and predicted CSEM data, consisting of the complex valued electric and magnetic fields measured at the detectors. MT predicted and observed data are in the form of field ratios or impedances, $\mathbf{Z}^{p}$ and $\mathbf{Z}^{obs}$. Diagonal weighting matrices, $\mathbf{D}_{CSEM}$ and $\mathbf{D}_{MT}$ are incorporated into the error functional to help compensate for noisy measurements. A successful outcome for imaging joint data also requires careful weighting between the CSEM and MT data types, otherwise one data type can predominate in the imaging process. Here we introduce the weighting coefficients α and β so that each data type makes a meaningful contribution in the imaging process. Our strategy for selecting α and β is based upon testing several trial values. Only a few inversion iterations are necessary to determine if the data sets are appropriately balanced. Other approaches to this problem can be found in [6]. Stabilization terms also appear in (1) and are designed

to treat media exhibiting transverse electrical anisotropy. Parameterization of anisotropic conductivity is made on a Cartesian mesh, where horizontal and vertical values are assigned to each cell in the mesh. Stabilization is achieved by reducing the model curvature in three dimensions in the minimization process. To do this we employ a FD approximation to the Laplacian (∇^2) producing a roughening matrix **W**. **W** acts on both the horizontal and vertical conductivity values $\mathbf{m_h}$ and $\mathbf{m_v}$, which are bounded using log or hyperbolic transformations. The regularization parameters, λ_h and λ_h control the amount of smoothing admitted into the model. Choice of the regularization parameters is dictated by the data noise and is optimally carried out using a cooling approach. We refer the reader to [10] for additional details. Minimization of (1) is carried out using a non-linear conjugate gradient scheme, ideal for large scale data and imaging volumes and parallelizes readily.

3. Imaging Examples

The Campos basin, located off shore of Brazil is a known oil and gas province with ongoing production. In 2004, a 3D CSEM survey was carried out to better quantify the hydrocarbon potential over part of the basin. The sail lines on a 40 x 40 km^2 grid used for subsurface conductivity mapping are shown at the top of Figure 2. Data was collected from nearly 1 million transmitter sites along the sail lines using 23 sea bottom detectors. Obviously, this amount of data cannot be treated with the current inversion methodology, even with a massively parallel implementation. Every source treated by the imaging algorithm requires a forward simulation, an adjoint computation, as well as two or more additional simulations in a line search for each nonlinear inversion update. To efficiently deal with the data volume, we use a general reciprocity principle that involves the interchange of transmitter and receiver points. Hence, the positions of the actual CSEM transmitter along the sail line become the computational receiver profiles, and the actual CSEM detectors on the seafloor become computational sources. The equivalent reciprocal problem involves 951,423 data points and 207 effective sources, since there are 23 source locations with three polarizations and each operating at the three discrete excitation frequencies of 0.125 Hz, 0.25 Hz, and 0.5 Hz. Each effective transmitter is polarized according to the antenna orientation of its corresponding detector.

Analysis of the Campos Basin data without taking anisotropy into account produced serious image artifacts [11], where the data were analyzed using 32,768 tasks/processors on the IBM Watson Research Blue Gene/L supercomputer over a 24 hour period. Even though the imaging result was deemed an initial failure it pointed to the correct approach to analyzing the data. Subsequent data analysis by [7] incorporating formation anisotropy produced interpretable results (Figure 2). It is also important to stress the need for fast processing times in imaging CSEM data in three dimensions. Initial imaging experiments required over four months of processing time on distributed clusters based on Intel or AMD processors utilizing 1024 tasks on an InfiniBand fabric.

An important exploration problem to demonstrate the advantages of joint conductivity inversion of CSEM and MT data is the imaging of oil bearing horizons in the presence of sub salt structures. The geometries of the reservoirs and salt structures are exceedingly difficult to map without recourse to 3D imaging. Such structures are encountered in the Gulf of Mexico, where seismic imaging beneath salt can be a formidable task. For oil bearing horizons above salt, the situation is better, but we will show that such structures can be identified much better under a joint CSEM/MT imaging framework.

In this synthetic imaging example, the data consists of 143 MT stations spread over a 25 × 25 km^2 grid with a 2.5 km sampling interval. Each of the two impedance tensor elements Z_{xy} and Z_{yx} is measured for 13 MT frequencies, ranging (logarithmically) from $5 \cdot 10^{-4} - 0.125$ Hz. The grid of CSEM detectors is a sub grid of the MT station grid, with 63 locations comprising an area of 20×15 km^2. As mentioned previously, it is common to treat marine CSEM data in a reciprocal way, owing to the enormous data volumes generated with a continuously moving transmitter towed by the vessel. Thus with two CSEM frequencies, 0.25 and 0.75 Hz, we simulate a total of 126 sources. A total of 6468 in-line receivers are

evenly spread over the actual seven CSEM sail lines. These lines are 50 m above the sea floor and are spaced at 2.5 km intervals. Counting in-phase and quadrature components of the complex data, the total number of CSEM and MT data points are 12,936 and 7436, respectively. More details regarding the data acquisition geometry and model can be found in [4].

The image results of the separate CSEM and MT inversions are shown in Figure 3 and clearly illustrate the different degrees of resolution achieved by either method. While the oil bearing horizon is indicated by the CSEM image, it does not provide a clear delineation of its shape. On the other hand, the MT data is only sensitive to the large salt bodies, where the MT image shows salt body conductivities which are generally above the true values. A great improvement is achieved by the joint inversion (d), both in terms of delineation of the reservoir and salt bodies, as well as in reproducing the true conductivities. Note also that the depth of the salt bodies is reproduced to a fairly good degree. To image the different scenarios, 7,875 tasks were employed on Franklin (Cray XT4) system at National Energy Research Scientific Computing Center (NERSC). Processing time for the different imaging experiments varied between 5 and 9 hours.

4. Acknowledgements

This work was carried out at Lawrence Berkeley National Laboratory, with base funding provided by the United States Department of Energy, Office of Basic Energy Sciences, under contract DE-AC02-05CH11231. Additional funding and support was provided by the ExxonMobil Corporation.

5. References

[1] Eidesmo T., Ellingsrud S., MacGregor L. M., Constable S., Sinha M. C, Johansen, S., Kong, F. N., Westerdahl, 2002, Sea Bed Logging (SBL), a new method for remote and direct identification of hydrocarbon filled layers in deepwater areas, First Break, 20.3, 144-152.

[2] Ellingsrud S., Eidesmo T., Johansen S., Sinha M. C., MacGregor, L. M, Constable, S., 2002, Remore sensing of hydrocarbon layers by seabed logging (SBL): Results from a cruise offshore Angola: The Leading Edge, **21**, 972-982.

[3] Constable, S., 2006, Marine electromagnetic methods – A new tool for offshore exploration: The Leading Edge 25, 438-444.

[4] Commer M., and Newman, G. A., 2009, Three-dimensional controlled-source electromagnetic and magnetotelluric joint inversion: Geophysical Journal International, *In Press*.

[5] Mackie, R. M., Watts, M. D. & Rodi, W., 2007. Joint 3D inversion of marine CSEM and MT data, *SEG Techn. Prg. Exp. Abstr. 26*, 574-578.

[6] Newman, G. A. and Commer, M., 2009, Imaging CSEM data in the presence of electrical anisotropy: submitted Geophysics.

[7] Carazzone J. J., Dickens T. A., Green, K. E., Jing, C., Wahrmund, L. A., Willen, D. E., Commer M., and Newman G. A., 2008, Inversion Study of a Large Marine CSEM Survey: Society of Exploration Geophysicists Expanded Abstracts, **27**, 644-647.

[8] Jing, C., K. E. Green, and D. Willen, 2008, CSEM inversion: Impact of anisotropy, data coverage, and initial models: 78th Annual International Meeting, SEG, Expanded Abstracts, 604-607.

[9] Commer M., and Newman, G. A., 2008, New advances in three-dimensional controlled-source electromagnetic inversion: Geophysical Journal International, **172**, 513-535.

[10] Newman, G. A., and Boggs, P. T., 2005, Solution accelerators for large-scale three-dimensional electromagnetic inverse problems: Inverse Problems, **20**, S151-S170.

[11] Commer M., Newman G. A., Carazzone J. J., Dickens T. A., Green K. E., Wahrmund L. A., Willen, D. E., Shiu J., 2008, IBM J. Res & Dev NO. ½, January/March 2008.

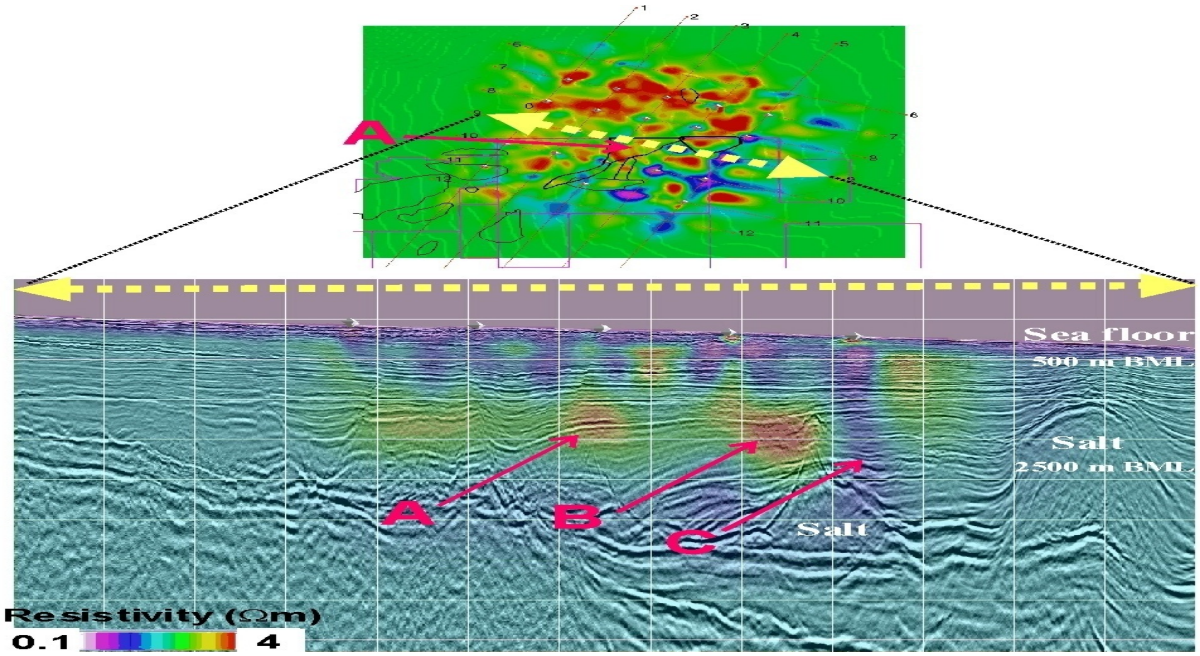

Figure 2. Rendered at the top is the average vertical resistivity map from 500 to 2500 m below the seafloor, superimposed with sail lines used to acquire the Campos Basin data. The cross-section at the bottom shows the vertical resistivity image along the indicated transect. The Campos Basin experiment demonstrated the necessity to incorporate electrical anisotropy into the imaging processes for accurate results. The CSEM image is shown together with seismic reflection horizons. Anomaly A is related to enhanced resistivity due to a known oil field. Anomaly B is enhanced resistivity and may indicate a possible hydrocarbon trap above a large salt body. Enhanced conductivity at C is likely to be related to conductive brines originating from salt below. Results presented by [7].

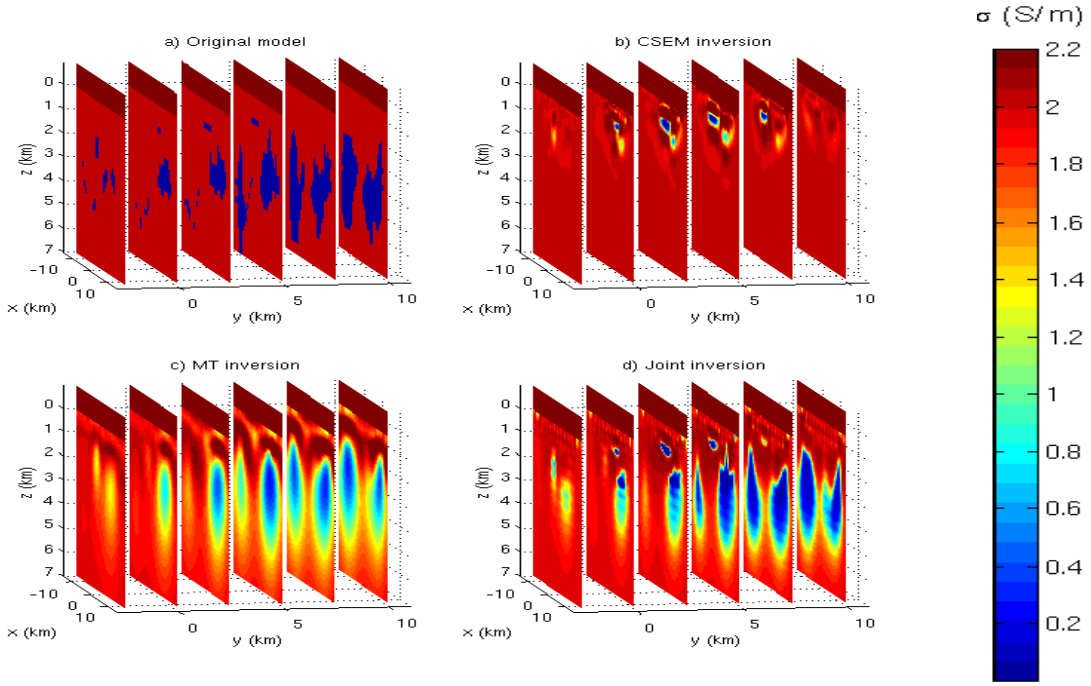

Figure 3. Marine prospecting study on joint CSEM and MT imaging showing original model (a), CSEM inversion (b), MT inversion (c), and joint inversion (d). Images are rendered in electrical conductivity.